

DEFOCUS DEBLUR MICROSCOPY VIA HEAD-TO-TAIL CROSS-SCALE FUSION

Jiahe Wang[†] Boran Han^{‡*}

[†] School of Computing and Information, University of Wisconsin-Madison, Madison, WI 53715

[‡] Shell International Exploration and Production Inc, Boston, MA 02210

ABSTRACT

Microscopy imaging is vital in biology research and diagnosis. When imaging at the scale of cell or molecule level, mechanical drift on the axial axis can be difficult to correct. Although multi-scale networks have been developed for deblurring, those cascade residual learning approaches fail to accurately capture the end-to-end non-linearity of deconvolution, a relation between in-focus images and their out-of-focus counterparts in microscopy. In our model, we adopt a structure of multi-scale U-Net without cascade residual leaning. Additionally, in contrast to the conventional coarse-to-fine model, our model strengthens the cross-scale interaction by fusing the features from the coarser sub-networks with the finer ones in a head-to-tail manner: the decoder from the coarser scale is fused with the encoder of the finer ones. Such interaction contributes to better feature learning as fusion happens across decoder and encoder at all scales. Numerous experiments demonstrate that our method yields better performance when compared with other existing models.

Index Terms— Microscopic Imaging, Defocus Deblurring, Deep learning, Feature Fusion, Multi-scale Feature

1. INTRODUCTION

The quality of images taken by microscopes is imperative to biology-related research as well as disease diagnoses, such as malaria and cancer detection. However, keeping the biology sample of the target in focus can be challenging due to the imperfect microscopy’s mechanical stability. The drift caused by instability is called mechanical drift [1]. While lateral drift (x and y direction) can be corrected by image registration [2], drift along the axial axis (z-direction) poses a significant challenge in correction. If not corrected, such drift can decrease the resolution of microscopic imaging. In the case of microscopes with a high-precision objective lens, samples taken at $1 \mu\text{m}$ away from the focal plane can lead to tremendous image quality degradation. However, such a high-precision objective lens can be essential for single-molecule tracking and molecule biology research.

A conventional solution includes improving mechanical stability [3] or installing a real-time feedback system, such as

focus lock [1]. One prevalent method is to make an infrared beam reflected off a cover-slip and calculate the shifts in the position of this beam to maintain constant objective-slide separation by closed-loop control. However, such a method is also found to be vulnerable when correcting significant drift. In addition, out-of-focus (OOF) images can be wasted if mechanical drift can’t be corrected since such an inconvenient issue will lead to data re-acquisition.

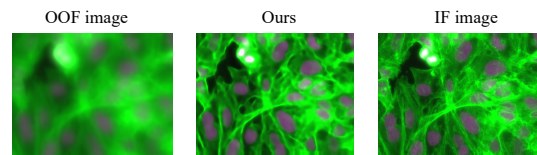


Fig. 1. Example OOF image (left), predicted IF images from our method (middle) and ground truth IF images (right)

An alternative solution to avoid data re-acquisition is to deblur the OOF image using image processing methods. Traditionally, deconvolution has been implemented to recover the in-focus (IF) images from OOF images [4]. This method usually requires to have point spread function (PSF) [4]. However, in practice, finding the true PSF is impossible. Therefore, an approximation of PSF is usually obtained by theoretical calculation based on the numerical aperture (N. A.) or measurement from some known probes (i. e., beads). Recently, defocus deblurring using deep learning has become a popular topic thanks to convolution neural networks (CNN). Such methods are most commonly used to process blurred pictures taken by cameras [5, 6]. In contrast to the conventional imaging system, i.e., camera, the microscopic image is often required to be accurate. Despite the fact that limited methods have been introduced focuses on solving the deblurring problems for microscopy images [7, 8, 9, 10, 11], some of the methods are tested under synthetic defocus data [11, 7], while others either fail to provide an end-to-end method [8]

To overcome these limitations, we develop an end-to-end deep learning-based workflow to predict IF microscopic images from OOF counterparts. Inspired by [12], we adopt a multi-scale U-Net, with feature fusion across scales in a head-to-tail manner. We test two fusion modes and demonstrate that

*Corresponding author.

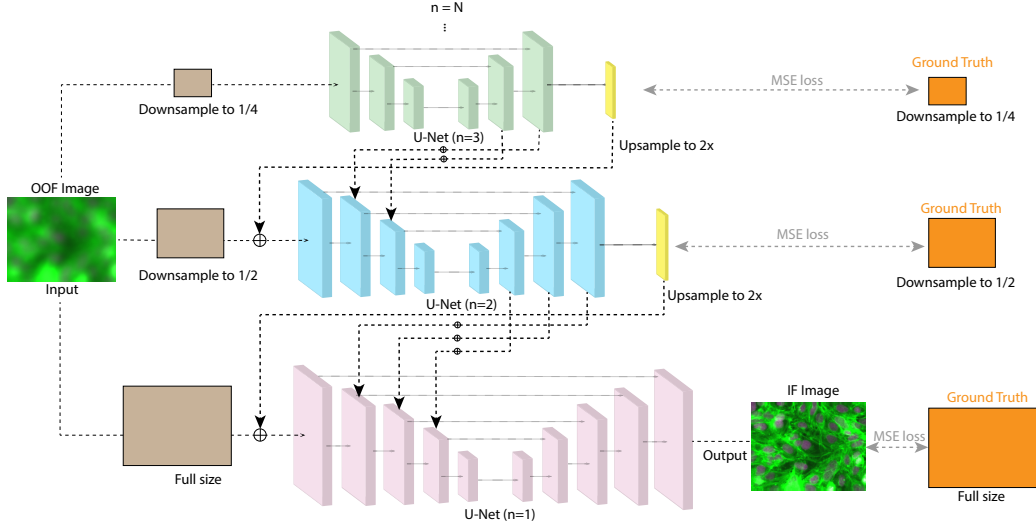


Fig. 2. The structure of our model. OOF images will be down-sampled and fed into corresponding multi-scale U-Net. The hidden features from the decoder of coarser sub-networks will be fused to the encoder of the finer sub-networks (marked as symbol \oplus), improving the training efficiency.

our proposed architecture performs better than other competing methods.

2. METHOD

2.1. Prior knowledge

Problem defined. An OOF image (x) can be obtained from IF image (y) convoluted by the PSF at a given z :

$$x = y * PSF(z) + \epsilon \quad (1)$$

where $*$ is the convolution operator and ϵ is the noise. To obtain y from x , an inverse operator of convolution is needed, i. e. deconvolution.

Coarse-to-fine network. As a pioneering work, [12] directly learns the relation between blurry-sharp image pairs in an end-to-end manner by adopting a coarse-to-fine strategy. Each subnetwork consists of a sequence of convolutional layers that maintains the spatial resolution of input feature maps. Different scales of input images are fed into the corresponding sub-networks. The resultant image from a coarser scale sub-network is added to the input of a finer scale sub-network to enable coarse-to-fine information transfer. The reconstruction procedure of [12] is formulated as follows [13]:

$$\hat{y}_n = U_{\theta_n}^{(n)}(x_n; \hat{y}_{n+1} \uparrow) + x_n \quad (2)$$

where $U_{\theta_n}^{(n)}$ is the n -th subnetwork parameterized by θ_n . \hat{x}_n and \hat{y}_n are blurred and predicted deblurred images at n -th scale. \uparrow is the upsampling operation. It is based on the assumption

that the deblurred image can be obtained by adding the fine details to the blurred images (Eq. 2).

However, such an assumption is inaccurate in the microscopy system, as such scheme adopts a linear summation of iterative nonlinear correction, following the minor perturbation manner. However, the inverse operation of Eq. 1 (deconvolution) is the end-to-end nonlinear relation between x and y . Accordingly, in the following section, we proposed a model $M : x \rightarrow y$ that captures the non-linearity of deconvolution while preserving the coarse-to-fine multi-scale strategy.

2.2. Defocus deblurring model

We exploit U-Net [14] of each sub-network[15]. However, instead of learning the finer residual of the images and adding to the blurred images, we fuse distilled information between hidden layers between the adjacent sub-networks. Such a feature fusion has been shown to boost the representation power of CNNs, such as Residual Networks (ResNet) [16]. In our model, the output of n -th sub-network is obtained from blurred images x_n and the output of $n + 1$ -th sub-network, \hat{y}_{n+1} . n -th sub-network ($U_{(\theta_n, \theta_{n+1})}^{(n)}$) is parameterized by θ_n and θ_{n+1} when $n < N$:

$$\hat{y}_n = U_{(\theta_n, \theta_{n+1})}^{(n)}(x_n; \hat{y}_{n+1} \uparrow) \quad (3)$$

and is parameterized by θ_n when $n = N$

$$\hat{y}_n = U_{(\theta_n)}^{(n)}(x_n) \quad (4)$$

where N is the number of scales, or subnetworks. $U^{(n)}$ denotes the encoder-decoder-based U-Net with symmetric skip

Distance		34 μm	28 μm	22 μm	16 μm	10 μm	No. of trainable parameters
$N = 1$ (U-Net)	PSNR	34.013	34.868	36.182	36.455	38.409	1,942,962
	SSIM	0.8482	0.8737	0.9013	0.9260	0.9561	
Summation fusion							
$N = 2$	PSNR	33.608	35.122	35.582	37.399	38.991	1,986,116
	SSIM	0.8451	0.8753	0.8989	0.9295	0.9591	
$N = 3$	PSNR	34.641	35.619	36.418	37.474	39.831	2,543,478
	SSIM	0.8454	0.8706	0.8990	0.9263	0.9576	
$N = 4$	PSNR	34.552	35.688	36.352	37.993	40.860	2,569,512
	SSIM	0.8491	0.8721	0.8978	0.9309	0.9612	
Concatenation fusion							
$N = 2$	PSNR	34.212	35.086	34.361	37.407	38.932	1,986,116
	SSIM	0.8462	0.8708	0.8907	0.9265	0.9529	
$N = 3$	PSNR	33.928	35.402	36.298	37.914	39.725	2,543,478
	SSIM	0.8452	0.8702	0.8983	0.9296	0.9589	
$N = 4$	PSNR	34.782	35.596	36.448	37.591	40.583	2,942,760
	SSIM	0.8487	0.8708	0.8996	0.9299	0.9602	

Table 1. PSNR and SSIM values of our model with different number of scales (N) and feature fusion modes. Best in bold.

connections that directly transfers the feature maps from the encoder to the decoder. In contrast to conventional U-Net, the encoder $U^{(n)}$ of our model is also connected with the decoder of $U^{(n+1)}$, shown in Figure 2. Intuitively, our finer model can enable more efficient learning via utilizing the knowledge distilled from coarser counterparts. In detail, the $U^{(n)}$ can be represented as $(E_0^{(n)}, E_1^{(n)}, \dots, E_i^{(n)}, \dots, E_I^{(n)})$ and $(D_0^{(n)}, D_1^{(n)}, \dots, D_i^{(n)}, \dots, D_I^{(n)})$, where $E_i^{(n)}$ and $D_i^{(n)}$ are i -th features maps in the encoder and decoder of $U^{(n)}$, respectively. As a result, $E_i^{(n)}$ can be obtained by the following equation:

$$E_i^{(n)} = F(E_i^{(n)}, D_{i-1}^{(n+1)}) \quad (5)$$

F is the feature fusion operator which takes the $E_i^{(n)}$ and $D_{i-1}^{(n+1)}$.

We use the multi-scale loss function, defined as follows:

$$L = \sum_{n=1}^N (\hat{y}_n - y_n)^2 \quad (6)$$

where y_n is the down-sampled ground-truth. By this mean, the output from each scale is constrained by the ground truth, ensuring that the features are correctly trained before fusion.

2.3. Directional Feature Fusion

We here apply two methods to fuse hidden features: summation and concatenation. In residual learning mode, the learnt features from decoder layer in $n + 1$ subnetwork ($D_{i-1}^{(n+1)}$) are added to encoder layer of n subnetwork ($E_i^{(n)}$):

$$E_i^{(n)} = E_i^{(n)} + D_{i-1}^{(n+1)} \quad (7)$$

Alternatively, $E_i^{(n)}$ can also be obtained by channel aware concatenating the $D_{i-1}^{(n+1)}$:

$$E_i^{(n)} = [E_i^{(n)} : D_{i-1}^{(n+1)}] \quad (8)$$

where $:$ is the concatenation operator. The above equation (Equation 8) depicts feature concatenation mode. Our proposed fusion is directional: decoder features from coarser scale sub-network are fused to the encoder from finer scale sub-network.

3. EXPERIMENTS

3.1. Experiment Settings

Dataset. Our data sets come from the Broad Bioimage Benchmark Collection [17] (<https://bbbc.broadinstitute.org/BBBC006>). The data sets consist of 34 sets of microscopic images from human U2OS cells. The cells are stained with Hoechst 33342 markers and actin markers by phalloidin.

The stained cells are imaged with an exposure of 15 and 1000 ms for two colors sequentially using a 20x objective. For each site, the optimal focus is found via laser auto-focusing. The automated microscope was then programmed to collect a z-stack of 32 image sets with the step size of 2 μm . As instructed by the dataset, we set $z = 17$ as our ground truth. Each z position consists of 768 images from different imaging areas. Each image, containing two-color channels, has a size of 696 x 520 pixels in 16-bit TIF format. In our experiment, we assign the first 675 pictures as the training set and the rest

Distance	Metric	34 μm	28 μm	22 μm	16 μm	10 μm	No. of trainable parameters
Input	PSNR	32.048	32.421	32.915	33.732	35.404	N/A
	SSIM	0.7161	0.7572	0.7861	0.8300	0.8954	
Nah et. al. [12]	PSNR	32.810	33.705	35.172	36.419	37.763	1,772,740
	SSIM	0.8337	0.8616	0.8934	0.9253	0.9552	
Liu et. al. [9]	PSNR	31.011	32.872	34.030	35.098	37.199	1,461,124
	SSIM	0.7171	0.7704	0.8442	0.9051	0.9469	
Na et. al. [10]	PSNR	31.409	31.908	32.513	34.804	37.253	4,384,262
	SSIM	0.7283	0.7586	0.8074	0.8908	0.9407	
Zhao et. al. [7]	PSNR	34.125	35.153	36.412	37.995	40.420	811,778
	SSIM	0.8260	0.8643	0.8952	0.9285	0.9612	
Ours (Summation fusion)	PSNR	34.552	35.688	36.352	37.993	40.860	2,569,512
	SSIM	0.8491	0.8721	0.8978	0.9309	0.9612	
Ours (Concatenation fusion)	PSNR	34.782	35.596	36.448	37.591	40.583	2,942,760
	SSIM	0.8487	0.8708	0.8996	0.9299	0.9602	

Table 2. PSNR and SSIM values of our model and other existing models. Best in bold.

93 images as the test set. We segment each image into four images with the size of 348 x 260 for ease of computation.

Training and evaluation We use an Adam optimizer with a learning rate of 0.01, a momentum of 0.9, and a batch size of 8. The network is trained for 80 epochs. Because the PSF is depth-dependent, our model is trained from scratch for every depth for evaluation. For a fair comparison, all other competing methods are trained following the same process. SSIM and PSNR [18, 19] are measured for performance estimation. The following experiments were performed on a desktop with NVIDIA RTX 3080 GPU.

3.2. Experiment Results

Ablation study. We evaluate our model using a various number of sub-networks ($N = 1 - 4$) and notice that performance improves as N increases. The result of the 2-level U-Net performs only slightly better than the original U-Net model. However, when we added the third and fourth levels of the U-Net, the model’s performance increased substantially. This result could be proven by the PSNR and SSIM values shown in Table 1. We also assess the two feature fusion modes proposed in Section 2.3. Our results demonstrate that the summation mode performs slightly better than the concatenation mode. Additionally, the summation mode contains less trainable parameters.

Performance against other methods. To demonstrate our approach is able to accurately predict IF images, we compare our method with other existing methods, including methods from Nah et al. [12], Liu et al. [9], Na et al. [10] and Zhao et al. [7]. Among them, the study from Nah et al. [12] has been demonstrated using camera images, such as GoPro and Kohler Dataset. At the same time, the rest are specifically designed for the optical or electron microscopic imaging domain. We also note that not all methods provide source codes. Therefore, we implement their models based on the information provided

in the original papers. Liu et al. [9] use residual connections for denoising and deblurring; Na et al. [10] employ the multi-scale network consisting of several ResNet [16]; Zhao et al. [7] adopt the residual DenseNet (RDN) [20], which is commonly used for super-resolution imaging. Table 2 shows that our proposed method ($N = 4$) can predict the IF images more accurately. Additionally, we measured the SSIM and PSNR between the input and the label, serving as the baseline. The increase beyond baseline demonstrates the capability of image restoration using deep learning models.

4. CONCLUSION AND DISCUSSION

This paper develops a new coarse-to-fine network with head-to-tail feature fusion learning for microscopic image defocus deblurring. Our method shows superior results when tested with fluorescent images.

Advantages compared to coarse-to-fine multi-scale network [12] and other feature fusion-based modified models [21, 22]. Our model, describes in Eq. 4, depicts an end-to-end non-linear function between x and y via coarse-to-fine hidden feature learning ($E_i^{(n)}$). However, most of the existing networks [12, 21] learn the final output through a residual cascade manner (Δy). Another difference stems from our head-to-tail interaction between adjacent sub-networks. This unique interaction enables feature fusion between the decoding features of the coarser scale sub-network and encoding features of the finer scale sub-network. The fused features can be efficiently learned through another encoder-decoder within the same scale sub-network, which can be advantageous compared with conventional cross-layer feature fusion [22].

For future study, our head-to-tail interaction can also be potentially combined with attention gates. Additionally, we note that the performance of our method in other imaging domains awaits further evaluation.

5. REFERENCES

- [1] Ashley R. Carter, Gavin M. King, Theresa A. Ulrich, Wayne Halsey, David Alchenberger, and Thomas T. Perkins, “Stabilization of an optical microscope to 0.1 nm in three dimensions,” *Appl. Opt.*, vol. 46, no. 3, pp. 421–427, Jan 2007.
- [2] Ching-Wei Wang, Shuk-Man Ka, and Ann Chen, “Robust image registration of biological microscopic images,” *Scientific reports*, vol. 4, pp. 6050, 08 2014.
- [3] Azeem Ahmad, Vishesh Dubey, Ankit Butola, Balpreet Singh Ahluwalia, and Dalip Singh Mehta, “Highly temporal stable, wavelength-independent, and scalable field-of-view common-path quantitative phase microscope,” *Journal of Biomedical Optics*, vol. 25, no. 11, pp. 116501, 2020.
- [4] Jean-Baptiste Sibarita, *Deconvolution Microscopy*, pp. 201–243, Springer Berlin Heidelberg, Berlin, Heidelberg, 2005.
- [5] Junyong Lee, Hyeongseok Son, Jaesung Rim, Sunghyun Cho, and Seungyong Lee, “Iterative filter adaptive network for single image defocus deblurring,” in *The IEEE Conference on Computer Vision and Pattern Recognition (CVPR)*, June 2021.
- [6] Junyong Lee, Sungkil Lee, Sunghyun Cho, and Seungyong Lee, “Deep defocus map estimation using domain adaptation,” in *The IEEE Conference on Computer Vision and Pattern Recognition (CVPR)*, June 2019.
- [7] Huangxuan Zhao, Ziwen Ke, Ningbo Chen, Songjian Wang, Ke Li, Lidai Wang, Xiaojing Gong, Wei Zheng, Liang Song, Zhicheng Liu, Dong Liang, and Chengbo Liu, “A new deep learning method for image deblurring in optical microscopic systems,” *Journal of Biophotonics*, vol. 13, no. 3, pp. e201960147, 2020.
- [8] Yichen Wu, Yair Rivenson, Hongda Wang, Yilin Luo, Eyal Ben-David, Laurent Bentolila, Christian Pritz, and Aydogan Ozcan, “Three-dimensional virtual refocusing of fluorescence microscopy images using deep learning,” *Nature Methods*, vol. 16, 12 2019.
- [9] Jiahao Liu, Xiaoshuai Huang, Liangyi Chen, and Shan Tan, “Deep learning-enhanced fluorescence microscopy via degeneration decoupling,” *Opt. Express*, vol. 28, no. 10, pp. 14859–14873, May 2020.
- [10] Juwon Na, Gyuwon Kim, Seong-Hoon Kang, Se-Jong Kim, and Seungchul Lee, “Deep learning-based discriminative refocusing of scanning electron microscopy images for materials science,” *Acta Materialia*, vol. 214, pp. 116987, 2021.
- [11] Cheng Jiang, Jun Liao, Pei Dong, Zhaoxuan Ma, De Cai, Guoan Zheng, Yueping Liu, Hong Bu, and Jianhua Yao, “Blind deblurring for microscopic pathology images using deep learning networks,” *CoRR*, vol. abs/2011.11879, 2020.
- [12] Seungjun Nah, Tae Hyun Kim, and Kyoung Mu Lee, “Deep multi-scale convolutional neural network for dynamic scene deblurring,” in *The IEEE Conference on Computer Vision and Pattern Recognition (CVPR)*, July 2017.
- [13] Sung-Jin Cho, Seo-Won Ji, Jun-Pyo Hong, Seung-Won Jung, and Sung-Jea Ko, “Rethinking coarse-to-fine approach in single image deblurring,” in *The IEEE Conference on Computer Vision and Pattern Recognition (CVPR)*, 2021.
- [14] Olaf Ronneberger, Philipp Fischer, and Thomas Brox, “U-net: Convolutional networks for biomedical image segmentation,” *CoRR*, vol. abs/1505.04597, 2015.
- [15] Hongyun Gao, Xin Tao, Xiaoyong Shen, and Jiaya Jia, “Dynamic scene deblurring with parameter selective sharing and nested skip connections,” in *Proceedings of the IEEE/CVF Conference on Computer Vision and Pattern Recognition (CVPR)*, June 2019.
- [16] Kaiming He, Xiangyu Zhang, Shaoqing Ren, and Jian Sun, “Deep residual learning for image recognition,” in *2016 IEEE Conference on Computer Vision and Pattern Recognition (CVPR)*, 2016, pp. 770–778.
- [17] Vebjorn Ljosa, Katherine Sokolnicki, and Anne Carpenter, “Annotated high-throughput microscopy image sets for validation,” *Nature methods*, vol. 9, pp. 637, 06 2012.
- [18] Zhou Wang, A.C. Bovik, H.R. Sheikh, and E.P. Simoncelli, “Image quality assessment: from error visibility to structural similarity,” *IEEE Transactions on Image Processing*, vol. 13, no. 4, pp. 600–612, 2004.
- [19] Alain Horé and Djemel Ziou, “Image quality metrics: Psnr vs. ssim,” *2010 20th International Conference on Pattern Recognition*, pp. 2366–2369, 2010.
- [20] Yulun Zhang, Yapeng Tian, Yu Kong, Bineng Zhong, and Yun Fu, “Residual dense network for image super-resolution,” 2018.
- [21] Dong Hang, Pan Jinshan, Hu Zhe, Lei Xiang, Zhang Xinyi, Wang Fei, and Yang Ming-Hsuan, “Multi-scale boosted dehazing network with dense feature fusion,” in *CVPR*, 2020.
- [22] Yaowei Li, Ye Luo, Guokai Zhang, and Jianwei Lu, “Single image deblurring with cross-layer feature fusion and consecutive attention,” *Journal of Visual Communication and Image Representation*, vol. 78, pp. 103149, 2021.